Relativistic theory of pairing in infinite nuclear matter

M. Serra, A. Rummel, and P. Ring
Physik-Department der Technischen Universität München, D-85748 Garching, Germany
(Received 28 June 2001; published 6 December 2001)

Realistic nuclear interactions based on the exchange of mesons are used to investigate pairing properties of symmetric nuclear matter in the framework of a relativistic field theory. For the pairing gap at the Fermi surface we find good agreement with earlier nonrelativistic descriptions based on phenomenological density dependent interactions of Gogny. The differences at large densities are traced back to the different behavior of these forces at short distances. The wave function of the Cooper pair as well as the contributions of the various parts of the interactions to the pairing field are investigated.

DOI: 10.1103/PhysRevC.65.014304 PACS number(s): 21.65.+f, 21.30.Fe, 74.20.Fg

I. INTRODUCTION

Since it was recognized, already in the late 1950s, that a large number of striking experimental facts, such as, the dramatic reduction of the moments of inertia in rotating nuclei or the energy gap in the spectra of many even-even nuclei, can be understood by the fact that these nuclei are superfluid systems [1], it is common practice to include pairing correlations in open shell nuclei in the BCS approximation.

In most of such investigations rather simplified phenomenological forces are used in the particle-particle channel to describe pairing correlations leading to superfluidity [2]. Most common is the monopole pairing force, which acts only between pairs of particles coupled to angular momentum zero, the so-called Cooper pairs, or the surface delta interaction. The strength of these forces is usually adjusted in a phenomenological way to the experimental pairing gap obtained from odd-even mass differences. More sophisticated density dependent Hartree-Fock-Bogoliubov calculations are based on Gogny forces of Gaussian shape with a finite range [3] or on Skyrme forces with zero range and an appropriate cutoff in the pairing channel [4].

In fact, relatively little is known about the details of the effective particle-particle force in nuclei. Although it is very important to take into account pairing to reproduce a large number of experimental facts in nuclear spectroscopy, most of the data are not very sensitive to the detailed shape of the pairing force. Already the simple ansatz of a monopole pairing, which allows to smear out the Fermi surface, leads in most of the cases to satisfactory results.

This fact is in sharp contrast with the situation in the particle-hole channel, where many data, such as saturation, effective masses, compressibility, surface energy, and other specific properties of nuclear spectra depend in a very sensitive way on the underlying effective force. Many investigations have been carried out in this context and since 1950s it is known that the bare nucleon-nucleon interaction determined from scattering experiments cannot be used directly in Hartree-Fock calculations. Three-body forces, Brueckner correlations and possibly also relativistic effects have to be taken into account [5]. In any case, the effective forces applicable in the *ph* channel for Hartree-Fock calculations show a strong density dependence. In fact, phenomenological density dependent Hartree-Fock calculations based on Skyrme or Gogny forces as well as phenomenological relativistic mean field (RMF) calculations in the framework of the nonlinear Walecka model are extremely successful in describing and predicting many of the properties of finite nuclei over the entire periodic table [6].

In the particle-particle channel the situation is very different. From general considerations it follows that the effective pairing force should be also density dependent. In any case it should approach at low densities outside the nuclear surface the bare nucleon-nucleon interaction. Therefore, density dependent effective pairing forces that interpolate between the bare nucleon-nucleon interaction at low densities and an adjusted interaction in the nuclear interior have been used successfully for the description of the halo phenomena [7,8]. On the other side, one has also obtained good agreement with experimental halo densities by using the phenomenological Gogny interaction with finite range but no density dependence in the $T=1$ pairing channel [9]. In addition, very little is known about the range of the effective pairing force. Gogny has adjusted it to the properties of the G matrix calculated from bare nucleon-nucleon interactions. Pure zero range forces lead to a divergence of the gap equation. Hence, in all applications zero range pairing forces have been used either in finite configuration spaces or in connection [4] with a cutoff introducing in this way again a finite range. The size of this cutoff parameter is usually determined by heuristic arguments and in many cases just by the limitations of the computer.

To obtain a full understanding of pairing properties in nuclei, however, one should start with a realistic bare nucleon-nucleon interaction. Over the years it has often been emphasized that the effective force in the pairing channel is not necessarily the G matrix [10], which sums up all the ladder diagrams, but the K matrix that sums up all the irreducible diagrams [11]. Several investigations in this direction have been carried out in neutron matter [12], but the importance of such renormalization effects in the *pp* channel has so far not been discussed for symmetric nuclear matter. In fact, at least in the singlet channel with the quantum numbers $S=0$ and $T=1$, the renormalization does not seem to play an essential role. Although this fact is not fully clarified so far, strong support for this assumption is given by nonrelativistic investigations [13] using the bare Paris potential for BCS calculations in nuclear matter at various densities. In these

calculations quantitative agreement is found for the strength of pairing correlations at the Fermi surface with the phenomenological results deduced from Gogny forces, which are believed to present a proper description of pairing in finite nuclei [3].

Here we extend such investigations in the context of a relativistic pairing theory, which has been developed in analogy to the nonrelativistic one [14,15]. Using Greens functions methods and the factorization of Gorkov [16], relativistic Hartree-Fock-Bogoliubov (HFB) equations have been derived in full analogy to nonrelativistic HFB theory. However, an early investigation of the pairing problem of symmetric nuclear matter with the phenomenological parameter sets of the RMF theory [15] was completely unsuccessful: the calculated gap parameters at the Fermi surface exceeded the standard values obtained with the Gogny force by more than a factor of 3. The origin of this failure was the behavior of the pairing matrix elements at large momenta. In fact, these forces were adjusted only for Hartree calculations, i.e., only for momenta below the Fermi momentum. In order to obtain reasonable values for the gap parameter one, therefore, has used a cutoff also in the relativistic cases [15,17,18].

Of course, bare nucleon-nucleon interactions have a proper cutoff, determined by the scattering data at high energies. We, therefore, start with a relativistic version of the one-meson exchange potential adjusted to the scattering data by Machleidt [20] as interaction in the *pp* channel and solve the relativistic BCS equations in infinite symmetric nuclear matter [15,21] in order to study pairing properties of the superfluid symmetric nuclear matter in the $T=1$ channel.

This paper is organized as follows. In Sec. II we briefly introduce the relativistic BCS equations and we present the solution for the pairing gap at the Fermi surface. We compare our relativistic results with nonrelativistic calculations based on the Gogny force $D1$ [19]. In Sec. III we study some properties of pairing correlations, i.e, Cooper pair wave function and the coherence length, obtained by relativistic and nonrelativistic calculations. In Sec. IV we summarize our results and give a short conclusion.

II. THE PAIRING GAP AT THE FERMI SURFACE

As discussed in Refs. [15,21] the relativistic Hartree-Fock-Bogoliubov equations are of the form

$$\begin{pmatrix} h-m-\lambda & \Delta \\ -\Delta^* & -h^*+m+\lambda \end{pmatrix} \begin{pmatrix} U \\ V \end{pmatrix}_k = E_k \begin{pmatrix} U \\ V \end{pmatrix}_k , \tag{1}$$

where

$$h=\alpha\mathbf{p}+\beta\Sigma \tag{2}$$

is the Dirac operator with the relativistic mass operator

$$\Sigma_{ab}=m\delta_{ab}+\sum_{cd} V_{adbc}\rho_{cd}, \tag{3}$$

and Δ is the relativistic pairing field

$$\Delta_{ab}=\frac{1}{2}\sum_{cd} V_{adbc}\kappa_{cd}. \tag{4}$$

The density ρ_{ab} and the pairing tensor κ_{ab} are obtained from the HFB wave functions U_k and V_k

$$\rho_{ab}=\sum_k V_{ak}^* V_{bk} \tag{5}$$

$$\kappa_{ab}=\sum_k V_{ak}^* U_{bk}. \tag{6}$$

According to the *no-sea approximation* the sum over k runs only over quasiparticle states corresponding to particle solutions of the Dirac equation.

Since we are mainly interested in a relativistic description of the *pp* channel and because it can be argued that the main effects of the Fock terms of meson exchange potentials are already taken into account at the Hartree level in a phenomenological way, in the following, we neglect the exchange term in the mass operator Σ and obtain in this way the relativistic Hartree-Bogoliubov equations.

Diagonalizing the Dirac operator h and neglecting the off-diagonal matrix elements of the pairing field in this basis, the full HB equations can be decomposed into (2×2) matrices of BCS type as in the nonrelativistic case, i.e.,

$$\begin{pmatrix} \epsilon(k)-\lambda & \Delta(k) \\ \Delta(k) & -\epsilon(k)+\lambda \end{pmatrix} \begin{pmatrix} u(k) \\ v(k) \end{pmatrix} = E(k) \begin{pmatrix} u(k) \\ v(k) \end{pmatrix}, \tag{7}$$

where $\epsilon(k)$ are the eigenvalues of the Dirac operator h, $\Delta(k)$ are the diagonal matrix elements of the pairing field in the Dirac basis, and

$$E(k)=\sqrt{[\epsilon(k)-\lambda]^2+\Delta(k)^2} \tag{8}$$

are the quasiparticle energies in the BCS approximation.

In the case of nuclear matter we consider a particle with momentum k moving in classical fields S and V of scalar and vector mesons. We find the eigenvalue of the Dirac equation $\epsilon(k)$ in Eq. (1) is given by

$$\epsilon(k)=V+\sqrt{k^2+M^{*2}}, \tag{9}$$

in which the effective mass M^* and the vector field V read $M^*=M+S=M+g_\sigma\sigma$ and $V=g_\omega\omega$, respectively. The fields are determined by the meson equations of the nonlinear RMF model [22]

$$\sigma=-\frac{4g_\sigma}{m_\sigma^2}\int\frac{d^3k}{(2\pi)^3}\frac{M^*}{\sqrt{k^2+M^{*2}}}v^2(k)+g_2\sigma^2+g_3\sigma^3, \tag{10}$$

$$\omega=\frac{4g_\omega}{m_\omega^2}\int\frac{d^3k}{(2\pi)^3}v^2(k), \tag{11}$$

where $v^2(k)$ are BCS occupation numbers and λ is the Fermi energy related to the Fermi momentum k_F by

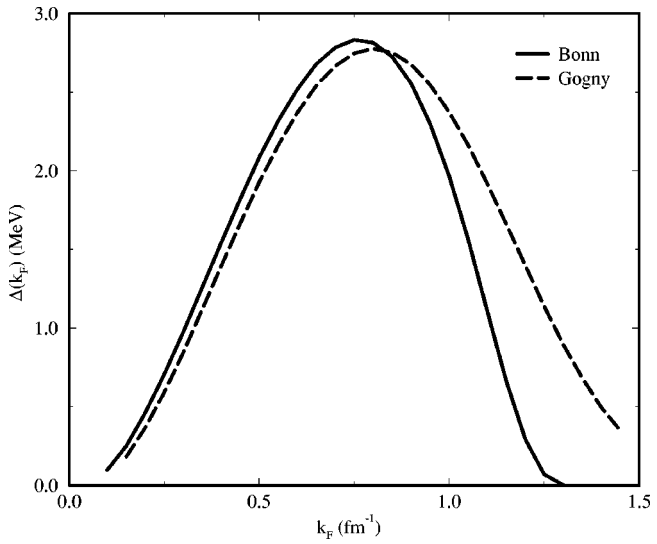

FIG. 1. Gap parameter at the Fermi surface Δ_F as a function of the density represented by the Fermi momentum k_F for the relativistic Bonn potential (version *B*) and for the Gogny force *D*1.

$$\lambda = V + \sqrt{k_F^2 + M^{*2}}, \tag{12}$$

and fixed by the density of the system $\rho = (m_\omega / g_\omega)^2 V$. In the following calculations the coupling constants g_σ, g_ω, g_2, and g_3, and the meson masses m_σ, m_ω are taken from the parameter set NL1 of the nonlinear RMF model [23]. However, the results for the pairing gap at the Fermi surface do not depend very much on the parameters used in the *ph* channel as long as one uses a parameter set that provides a successful description of the ground state properties of finite nuclei.

The pairing field $\Delta(k)$ obeys the usual gap equation

$$\Delta(p) = -\frac{1}{4\pi^2} \int_0^\infty v_{pp}(p,k) - \frac{\Delta(k)}{\sqrt{[\epsilon(k) - \lambda]^2 + \Delta^2(k)}} k^2 dk, \tag{13}$$

which is formally identical to the one in the nonrelativistic case. Here $v_{pp}(p,k)$

$$v_{pp}(p,k) = \int v_{pp}(\mathbf{p},\mathbf{k}) d\cos\theta \tag{14}$$

is the angle averaged relativistic *pp* interaction, θ being the angle between the vectors **p** and **k** (for details see Ref. [15]).

In this investigation we use the three relativistic versions *A*, *B*, and *C* of the Bonn potential discussed in Ref. [20]. They contain the exchange of several mesons. The details are given in the Appendix.

In Fig. 1 we display the resulting gap parameter Δ_F^B at the Fermi surface $\Delta_F = \Delta(k = k_F)$ as a function of the density represented by the Fermi momentum k_F for the relativistic Bonn-*B* potential (solid line) and compare it with the same quantity Δ_F^G obtained in a nonrelativistic calculation [19] based on the Gogny force *D*1 (dashed line). Apart from the difference at larger densities, the solutions are in excellent agreement. In both cases we find maximal pairing correlations of roughly 2.8 MeV at the Fermi momentum $k_F \approx 0.8\,\mathrm{fm}^{-1}$, i.e., at roughly one-fifth of nuclear matter density. As shown in Table I we find very similar results for the other relativistic forces Bonn *A* and Bonn *C*.

TABLE I. Maximal pairing correlations at the Fermi surface for the relativistic versions *A*, *B*, and *C* of the Bonn potential and for the Gogny force *D*1.

Potential	Δ_F (MeV)	k_F (fm^{-1})
Bonn *A*	2.80	0.76
Bonn *B*	2.84	0.76
Bonn *C*	2.83	0.76
Gogny *D*1	2.78	0.80

Since the pairing correlations are largest for small densities, i.e., at the surface of the nucleus, this result agrees with the usual observation that pairing in nuclei is a surface phenomenon. Moreover, the agreement between the results obtained with bare relativistic forces and those obtained with the Gogny force for the pairing properties of the symmetric nuclear matter is a particularly interesting outcome as in the latter case it has been shown [19] that using this density dependence of the gap parameter in semiclassical calculations the average pairing properties of finite nuclei can be reproduced rather well. Thus we can hope that this will remain true also for calculations in finite nuclei with bare relativistic interactions.

At saturation density ($k_F^S = 1.35\ \mathrm{fm}^{-1}$), it is rather difficult to decide whether nuclear matter is superfluid. In any case it seems to depend crucially on the interaction. For the Gogny force a small pairing gap of roughly 0.5 MeV is left, whereas for the Bonn-*B* potential there seems to be no pairing.

To understand the difference between Δ_F^B and Δ_F^G at higher densities, we analyze the behavior of $\Delta(k)$, $v_{pp}(k_F,k)$, and of the integrand of Eq. (13)

$$i(k) = -\frac{k^2}{4\pi^2} v_{pp}(k_F,k) \frac{\Delta(k)}{\sqrt{[\epsilon(k) - \lambda]^2 + \Delta^2(k)}} \tag{15}$$

for several values of k_F for both the interactions. Figures 2 and 3 show $v_{pp}(k_F,k)$, $\Delta(k)$, and $i(k)$ at $k_F = 0.3$ and 0.8 fm^{-1}, respectively, for which the agreement between the relativistic and the nonrelativistic solutions is good. Figure 4 shows the same quantities for $k_F = 1.2$ fm^{-1} for which Δ_F^B is much smaller than Δ_F^G. The graphs on the left refer to the relativistic calculations based on the Bonn-*B* potential and those on the right to the nonrelativistic calculations based on the Gogny force *D*1. We first consider the interactions $v_{pp}(k_F,k)$, plotted with dotted lines. The behavior of the Bonn potential differs considerably from that of the Gogny force. For small values of k_F (Figs. 2 and 3) the relativistic force is strongly attractive at small *k* and it becomes repulsive for large *k*. For larger values of k_F the strength of the attractive part decreases and for $k_F = 1.2$ fm^{-1} (see Fig. 4) the potential is only repulsive. On the contrary, the nonrela-

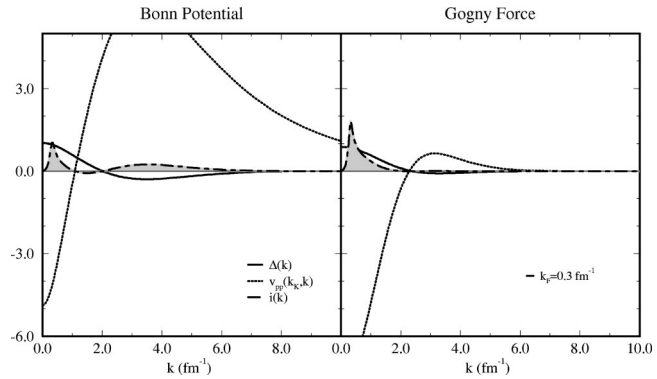

FIG. 2. Various contributions to the integral in the gap equation (13) for the density corresponding to the Fermi momentum $k_F = 0.3$ fm^{-1}. Comparison of the relativistic Bonn-*B* potential and the Gogny force. The details are discussed in the text.

tivistic force is attractive for nearly all momenta. The small repulsive part does not play an essential role here.

We next consider the pairing fields $\Delta(k)$ plotted with solid lines in Figs. 2–4. For $k_F = 0.3$ and 0.8 fm^{-1} $\Delta^B(k)$ and $\Delta^G(k)$ have comparable strengths, while for $k_F = 1.2$ fm^{-1} $\Delta^G(k)$ is far greater than $\Delta(k)^B$, as it is expected from the previous observations on the pairing gap at the Fermi surface.

Finally, we show the integrand $i(k)$ given in Eq. (15) by dot-dashed lines and we examine the different contributions of $v_{pp}(k_F,k)$ and $\Delta(k)$ to this integrand. The shaded areas represent the integral Δ_F. In the nonrelativistic case, for each value of k_F, Δ_F^G originates from the contributions of large intervals where the integrand is positive and of a negligibly small interval where the integrand is negative. In the relativistic case, the contributions of $\Delta(k)$ and $v_{pp}(k_F,k)$ to Δ_F^B depend on k_F. For $k_F = 0.3$ and 0.8 fm^{-1}, we find that three intervals contribute [24]. For $k_F = 1.2$ fm^{-1}, because v_{pp} is always positive, only two intervals of opposite sign contribute to Δ_F^B canceling each other to some extent and, therefore, reducing the pairing gap at the Fermi surface. In conclusion, the fact that Δ_F^B drops to zero faster Δ_F^G is due to the strong dependence of the Bonn potential on the Fermi momentum at large momenta, i.e., on the short distance behavior of the potential.

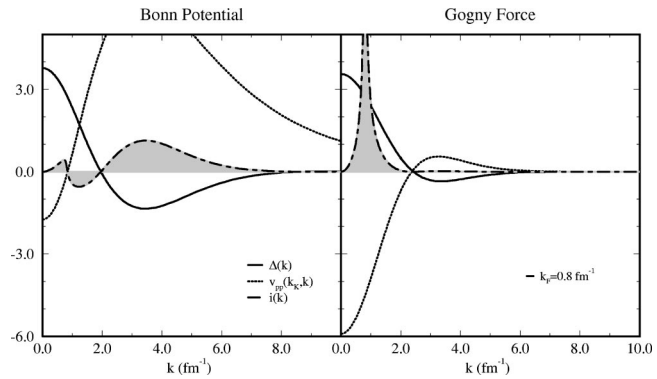

FIG. 3. The same results as in Fig. 2 for a Fermi momentum $k_F = 0.8$ fm^{-1}.

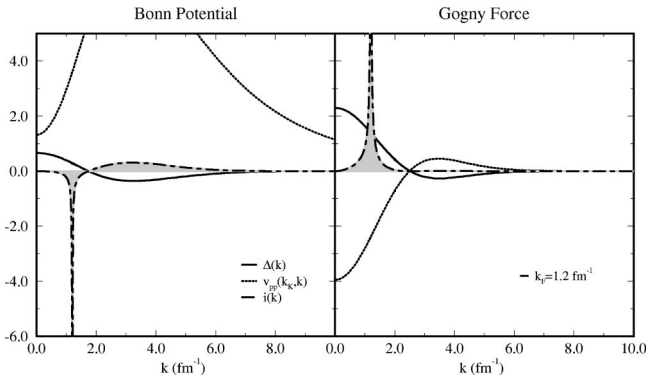

FIG. 4. The same results as in Fig. 2 for a Fermi momentum $k_F = 1.2$ fm^{-1}.

We now concentrate on the relativistic *pp* interaction. The Bonn potential [20] is defined as the sum of one-Boson-exchange contributions of six mesons, namely, σ, ω, π, ρ, δ, and η. In Fig. 5 we show the matrix elements $v_{pp}(k_F,k)$ of the Bonn-*B* potential together with the six contributions of the different mesons for $k_F = 0.8$ fm^{-1}. We observe that the full interaction results from the cancellation of two main terms: the negative contribution of σ meson and the positive contribution of the ω. Although the other mesons have much smaller contributions, they cannot be neglected because of the large cancellation between σ and ω. The influence of δ and η is however very small.

In Fig. 6 we study how the exchange of the different mesons contribute to the gap at the Fermi surface Δ_F. As we have just seen for the potential, this quantity results mainly from the exchange of σ and ω whose corresponding pairing gaps at the Fermi surface $\Delta_F^{\sigma,\omega}$ are of the order of $+9.5$ MeV and -6.8 MeV for maximal pairing correlations, respectively. The other mesons play a smaller role; among them we have $\Delta_F^{\pi} \approx -0.85$ MeV and $\Delta_F^{\rho} \approx +0.42$ MeV for the same

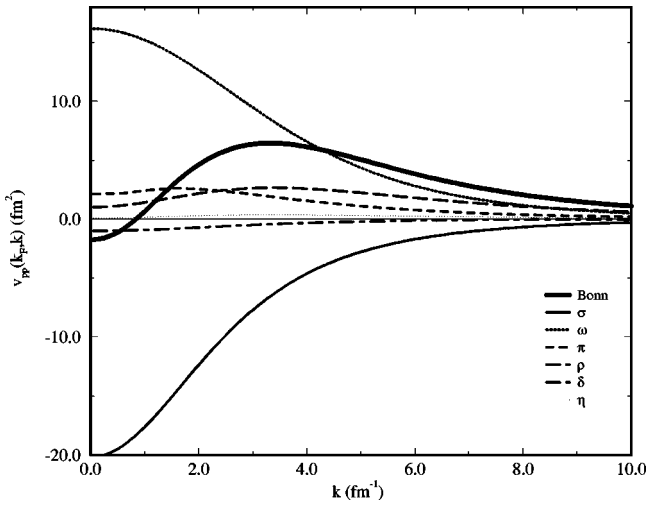

FIG. 5. Matrix elements of the relativistic Bonn-*B* potential in momentum space $v_{pp}(k_F,k)$ at the Fermi momentum of maximal pairing correlations $k_F = 0.8$ fm^{-1}. The thick solid line corresponds to the full potential and the thin lines correspond to the various one-meson exchanges.

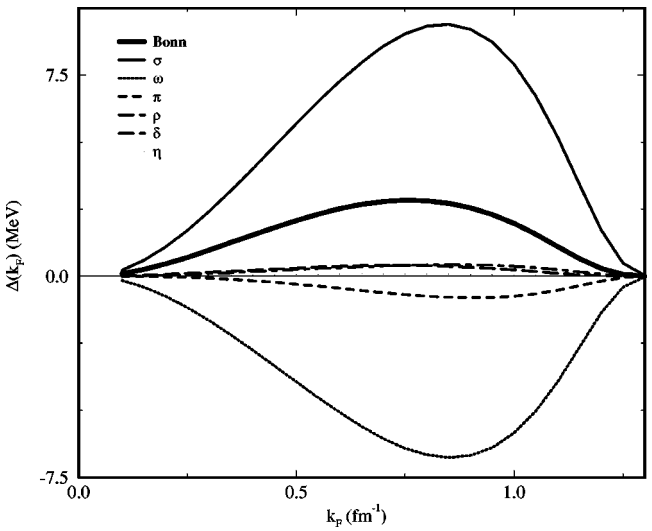

FIG. 6. Contributions of the different one-meson exchange potentials to the gap parameter at the Fermi surface as a function of the density represented by the Fermi momentum k_F. The thick solid line corresponds to the full gap and the thin lines correspond to the various mesons gaps.

value of k_F. The fact that the ρ-meson exchange gives a positive contribution to the total gap at the Fermi surface Δ_F^ρ is due to the tensor V_T and vector-tensor V_{VT} terms in the one-rho exchange potential (see Table II).

III. COOPER PAIR WAVE FUNCTION AND COHERENCE LENGTH

For a better understanding of the pairing properties we study the Cooper pair wave function. In momentum space it is defined by

$$\chi(k)=\frac{\Delta(k)}{2\sqrt{[\epsilon(k)-\lambda]^2+\Delta^2(k)}}. \tag{16}$$

On the left and on the right side of Fig. 7 we show $\chi(k)$ obtained with the Bonn potential and with the Gogny force, respectively, at the three values of k_F previously considered, i.e. $k_F=0.3$, 0.8, and 1.2 fm^{-1}. We observe that every wave

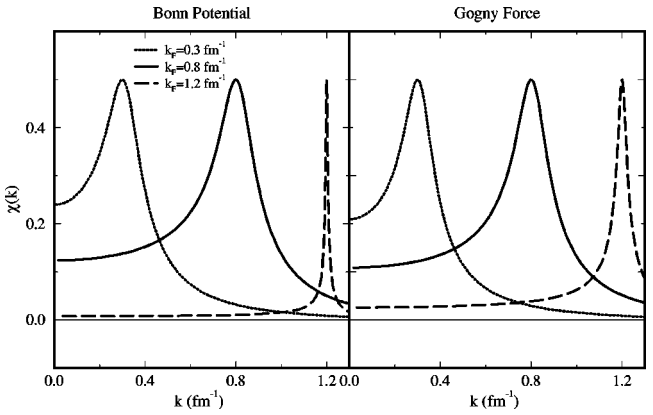

FIG. 7. Cooper pair wave functions in momentum space $\chi(k)$ calculated at different values of the Fermi momentum k_F as functions of the momentum k for the relativistic Bonn-B potential and for the Gogny force.

function is peaked at $k=k_F$. This is due to the fact that the denominator in Eq. (16) has a minimum at $k=k_F$, in fact it reduces to $\Delta(k_F)$.

The asymmetric behavior of the pair wave functions in the momenta intervals $k<k_F$ and $k>k_F$ is a consequence of the variation of the gap function $\Delta(k)$ with k. For both the interactions, the widths of the peaks, which represent the inverse of the coherence length, have the same size for $k_F=0.3$, and 0.8 fm^{-1}, while they are smaller for $k_F=1.2$ fm^{-1}. In addition, the fact that for $k_F=1.2$ fm^{-1} the width of the peak is narrower for the Bonn potential than for the Gogny force is consistent with the observation that in the former case the gap parameter at the Fermi surface Δ_F drops faster than in the latter. Apart from this, in momentum space there are no big differences between the wave functions $\chi(k)$ calculated with the relativistic and nonrelativistic forces.

Of particular interest is the wave function of the Cooper pair in coordinate space $\chi(r)$, where r represents the distance between the two nucleons forming a Cooper pair. It is obtained from $\chi(k)$ by Fourier transformation

$$\chi(r)=\int \frac{d^3k}{(2\pi)^3} e^{-i\mathbf{k}\cdot\mathbf{r}}\chi(k). \tag{17}$$

In Fig. 8 we plot this quantity for the Bonn potential and for the Gogny force at the three values of k_F used before. For

TABLE II. Functions $A_i(k,p)$, $B_i(k,p)$, and $C_i(k,p)$ of Eq. (A3).

i	Γ	χ_i	$A_i(k,p)$	$B_i(k,p)$	$C_i(k,p)$
σ	g_σ	$-g_\sigma^2$	$a(k,p)-m_\sigma^2$	$a(k,p)-\Lambda_\sigma^2$	
ω	$g_\omega\gamma^\mu$	$+g_\omega^2$	$b(k,p)$	$b(k,p)$	
π_{pv}	$(f_\pi/m_\pi)\gamma^5\gamma^\mu(k_\mu-p_\mu)$	$+(f_\pi/m_\pi)^2$	$p^2-k^2-m_\pi^2 a(k,p)$	$p^2-k^2-\Lambda_\pi^2 a(k,p)$	
ρ^V	$g_\rho\gamma^\mu$	$+g_\rho^2$	$b(k,p)$	$b(k,p)$	
ρ^T	$i(f_\rho/2M)[g_\rho\gamma^\mu(k_\nu-p_\nu)\sigma^{\nu\mu}]\vec{\tau}$	$-(f_\rho/2M)^2$	$[c(k,p)+m_\rho^2]m_\rho^2$	$[c(k,p)+\Lambda_\rho^2]\Lambda_\rho^2$	1
ρ^{VT}		$+2(f_\rho g_\rho/M)M^*$	m_ρ^2	Λ_ρ^2	
δ	$g_\delta\vec{\tau}$	$-g_\delta^2$	$a(k,p)-m_\delta^2$	$a(k,p)-\Lambda_\delta^2$	
η^{pv}	$(f_\eta/m_\eta)\gamma^5\gamma^\mu(k_\mu-p_\mu)\vec{\tau}$	$+(f_\eta/m_\eta)^2$	$p^2-k^2-m_\eta^2 a(k,p)$	$p^2-k^2-\Lambda_\eta^2 a(k,p)$	

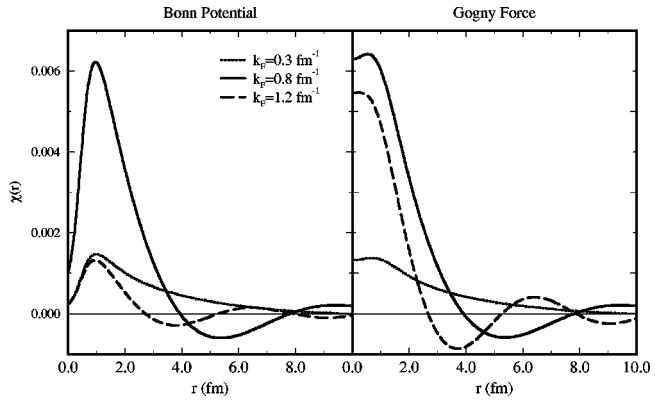

FIG. 8. Cooper pair wave functions in coordinate space $\chi(r)$ calculated at different values of the Fermi momentum k_F as functions of the coordinate r for the relativistic Bonn-B potential and for the Gogny force.

both interactions $\chi(r)$ are oscillating functions of r, and the oscillation rate increases with the density. However, we also observe important differences between the relativistic and the nonrelativistic calculations. In the former case, for all densities $\chi(r=0)$ is close to zero, then it increases till a maximum at $r_{\max}\approx 1.0$ fm and thereafter it starts to oscillate at different rates for each k_F. We observe that the highest maximum of the pair wave functions $\chi(r_{\max})\approx 0.0062$ fm^{-3} corresponds to the Fermi momentum for which pairing correlations are maximal, i.e., $k_F=0.8$ fm^{-1}. For $k_F=0.3$ and 1.2 fm^{-1}, we have $\chi(r_{\max})\approx 0.0015$ fm^{-3}.

In the case of the Gogny force, the situation is quite different. First of all, the pair wave functions $\chi(r)$ do not present any pronounced peak at small distances. In particular, they are almost constant in the interval $r<1.0$ fm for each k_F, then they decrease and they oscillate with an oscillation rate increasing with k_F as we have noticed already for the relativistic interaction. Comparing the strengths of $\chi^B(r)$ and $\chi^G(r)$ at the different densities, we observe that they are of the same order for $k_F=0.3$ and 0.8 fm^{-1}, for which, as it can be noticed from Fig. 1, also the agreement between the corresponding pairing gap at the Fermi surface is very good, namely, $\Delta_F^B(k_F=0.3\ \text{fm}^{-1})\approx\Delta_F^G(k_F=0.3\ \text{fm}^{-1})\approx 0.9$ MeV and $\Delta_F^B(k_F=0.8\ \text{fm}^{-1})\approx\Delta_F^G(k_F=0.8\ \text{fm}^{-1})\approx 2.8$ MeV. On the contrary, for $k_F=1.2$ fm^{-1} the strength of $\chi^G(r)$ is far greater than the strength of $\chi^B(r)$. This agrees with the fact that at this Fermi momentum the pairing gap obtained with the Gogny force is much greater than the pairing gap obtained with the Bonn potential, namely, we find $\Delta_F^G(k_F=1.2\ \text{fm}^{-1})\approx 1.9$ MeV and $\Delta_F^B(k_F=1.2\ \text{fm}^{-1})\approx 0.9$ MeV, respectively.

Let us now investigate which part of the interaction is responsible for pairing correlations? We, therefore, consider the Bonn potential in the coordinate space. In this case the Fourier transformation from momentum to coordinate space cannot be carried out analytically because of the presence of nonlocal terms [20]. We, therefore, have used a nonrelativistic reduction of the potential in the coordinate space, which is a good approximation of the relativistic one at small distances. In the upper part of Fig. 9, we show the even-singlet

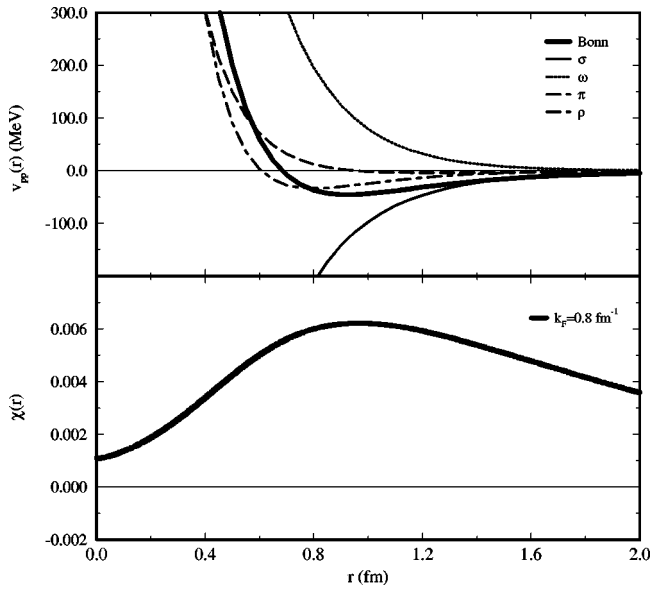

FIG. 9. Upper part: even-singlet central part of the Bonn potential in the coordinate space and its one-meson exchange contributions. The former is plotted with a thick solid line and the latter with thinner lines. Lower part: Cooper pair wave function at $k_F=0.8\,(\text{fm}^{-1})$. It is peaked where the interaction is mostly attractive.

($^1S_0$) central part of the bare interaction in coordinate space. We observe that the full potential, represented in the figure by a thick solid line, is repulsive at short distances, has a zero at $r\approx 0.7$ fm and then a minimum of the order of -50 MeV at $r_{\min}\approx 0.9$ fm and, finally, goes to zero for larger distances. The thinner lines represent the contributions of the various mesons. In particular, we notice the monotonic increasing and decreasing potentials corresponding to the attractive σ mesons and to the repulsive ω meson, the contribution of the one-pion exchange that in this channel of the pp interaction is strongly repulsive for $r\leqslant 1.0$ fm and weakly attractive for $r\geqslant 1.0$ fm, the rho-exchange potential, which is also strongly repulsive at small distances, has a zero at $r\sim 0.6$ fm and gives an attractive contribution of the order of -40 MeV at 0.8 fm, much stronger than the contribution of π. This is due to the fact that the ρ is heavier than the π meson and due to the presence of the tensor and vector-tensor terms in the potential. Moreover, the influence of the δ functions in the spin-spin (central) force of the one-pion and of the one-rho exchanges are reduced by the form factors applied to the nucleon-meson-nucleon vertices of the potential. In Fig. 9 we have omitted the contributions of the δ and η mesons as they are negligible.

In the lower part of Fig. 9 we show the Cooper pair wave function in coordinate space for $k_F=0.8$ fm^{-1} and observe a correspondence between behavior of the potential and the wave function: at small distances, where the interaction is strongly repulsive, the size of $\chi(r)$ is small. In particular, for interparticle distances less than 0.1 fm it seems very unlikely that two nucleons condense into a Cooper pair. At larger distances the strength of $\chi(r)$ clearly increases together with the decreasing in the strength of the potential, in particular, $\chi(r)$ has a maximum of 0.006 at $r_{\min}\approx 0.8$ fm at which the

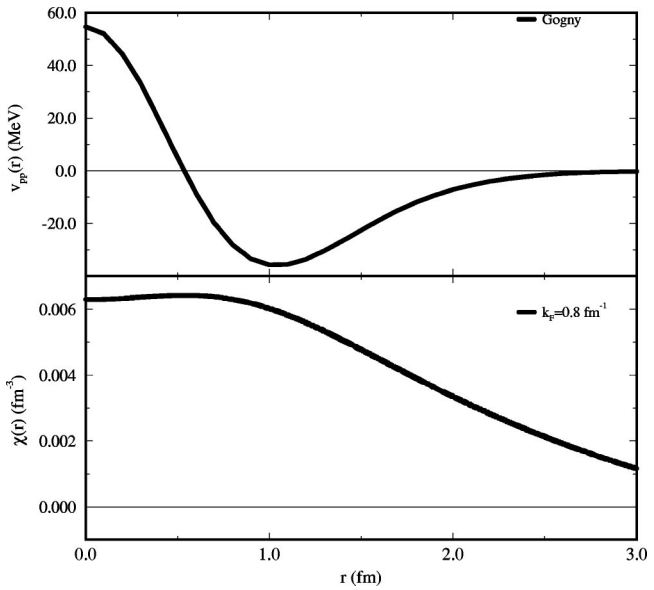

FIG. 10. Upper part: channel $^1S_0$ for the Gogny force in coordinate space. Lower part: Cooper pair wave function at $k_F = 0.8\,(\mathrm{fm}^{-1})$. It is maximal where the interaction is mostly repulsive.

interaction is mostly attractive. The same observations can be repeated also for the other values of the Fermi momentum, as we have seen that every Cooper pair wave function in coordinate space shows a peak at the same value $r = r_{\min}$ independent of the density.

From these considerations, we conclude that pairing correlations in nuclei are mainly due to the attractive part of the interaction and that the effect of the repulsive part is to shift the peak of the Cooper pair wave function outwards.

In Fig. 10 we show corresponding results in coordinate space for the Gogny force. In this case $\chi(r)$ is not suppressed by the repulsive part of the force, indeed its strength is maximal in the corresponding interval. In comparison with the Bonn potential, the Gogny force is far less repulsive at small distances and less attractive at intermediate distances.

An important quantity for a better understanding of pairing properties in nuclei is the coherence length ξ. From a microscopic point of view, it represents the squared mean distance of two paired particles. In terms of the Cooper pair wave functions it is defined as

$$\xi^2 = \frac{\int d^3r |\chi(\mathbf{r})|^2 r^2}{\int d^3r |\chi(\mathbf{r})|^2} = \frac{\int_0^\infty dk k^2 |\partial\chi(k)/\partial k|^2}{\int_0^\infty dk k^2 |\chi(k)|^2}, \qquad (18)$$

and for our calculations we have chosen the coordinate space representation since it is numerically more convenient. In Fig. 11 we display the coherence length ξ for the Bonn potential (solid line) and for the Gogny force (dashed line) as a function of k_F. In both cases, we observe that in the interval of larger pairing correlations, i.e., $0.4 \leqslant k_F\,(\mathrm{fm}^{-1}) \leqslant 0.9$ (see Fig. 1), ξ is an almost constant function of the Fermi momentum and has its lower value of around 5.0–6.0 fm. We,

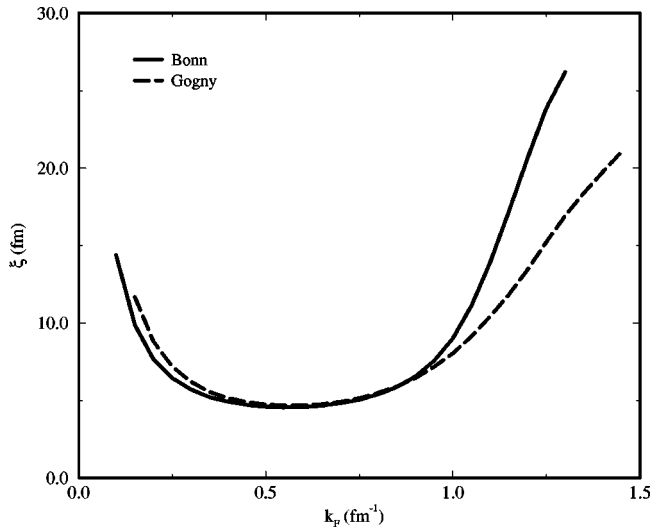

FIG. 11. Coherence length as a function of the Fermi momentum k_F for the relativistic Bonn-*B* potential and for the Gogny force.

therefore, find that the distance between two nucleons forming a Cooper pair is as large as the dimension of a nucleus. For low densities ($k_F \leqslant 0.25$ fm^{-1}) and for high densities ($k_F \geqslant 1.0$ fm^{-1}) the strength of the coherence length increases rapidly, meaning that the two nucleons become more and more separated. Finally the difference of the coherence length obtained with the Bonn potential and the coherence length calculated with the Gogny force at larger densities agrees with the observation that the pairing gap drops faster for the relativistic interaction than for the nonrelativistic force.

IV. CONCLUSIONS

In this work we applied a relativistic field theory to study pairing properties of symmetric nuclear matter in the $^1S_0$ channel at zero temperature. For this purpose, we have used the very successful nonlinear parametrization NL1 of the RMF theory in the *ph* channel, while the *pp* channel has been described for the first time by using a relativistic version of a realistic nucleon-nucleon interaction, namely, the Bonn potential.

In agreement with earlier nonrelativistic investigations based on the Paris potential, we have found that a relativistic bare nucleon-nucleon potential reproduces essentially the properties of nuclear matter obtained by using the phenomenological Gogny force, which is adjusted to reproduce experimental data of finite nuclei. We can hence conclude that renormalization effects of the pairing force do not play a major role in the $^1S_0$ channel. However, this observation is in contrast to results of calculations of polarization effects in pure neutron matter and this point deserves, therefore, further investigations.

In detail, we have found differences between the pairing properties calculated with the Bonn potential and the ones calculated with the Gogny force in the region of saturation density. By analyzing the origin of these discrepancies we have found that they originate from the strong repulsion in

the bare nucleon-nucleon interaction at short distances. It is to be expected that renormalization effects play a role to reduce these discrepancies.

Finally, we have calculated the contributions of the various meson exchange potentials to the pairing gap. As expected, there is a large cancellation between the strongly repulsive ω exchange and the strongly attractive σ exchange, which dominates the essential region of small momenta. The contributions of other mesons, such as the pion and the ρ, are much smaller, but not negligible because of this cancellation.

ACKNOWLEDGMENTS

We thank G. A. Lalazissis and D. Vretenar for valuable discussions. This work was supported in part by the Bundesministerium für Bildung und Wissenschaft under the Contract No. 06 TM 979.

APPENDIX

We give here the explicit expressions of the matrix elements entering the gap equation (13) of the relativistic Bonn potential, which, as already mentioned in the text, is defined as the sum of one-boson exchange of the mesons σ, ω, π, ρ, η, and δ. In momentum space, as shown in great detail in Ref. [15], the antisymmetrized matrix elements in the pp channel for one-meson exchange can be written as

$$v_{pp}(\mathbf{k},\mathbf{p}) = \mp\frac{M^{*2}}{2E^*(k)E^*(p)}\frac{\mathrm{Tr}(\Lambda_+(\mathbf{k})\Gamma\Lambda_+(\mathbf{p})\gamma^0\mathcal{T}^\dagger\Gamma^\dagger\mathcal{T}\gamma^0}{(\mathbf{k}-\mathbf{p})^2+m_m^2} \times f^2([\mathbf{k}-\mathbf{p}]^2), \tag{A1}$$

where $\Lambda_+(\mathbf{p})$ is the projector onto positive energy solution, $\mathcal{T}$ is the representation of the time reversal operator in Dirac space, and $f([\mathbf{k}-\mathbf{p}]^2)$ is the form factor applied to each nucleon-meson vertex, i.e.,

$$f([\mathbf{k}-\mathbf{p}]^2) = \left[\frac{\Lambda_m^2-m_m^2}{(\mathbf{k}-\mathbf{p})^2+\Lambda_m^2}\right], \tag{A2}$$

Λ_m being the cutoff mass. In Table II we list the vertex functions for the single one-meson exchange potential of the Bonn potential.

As we perform only pairing correlations in the $T=1$-channel, the dependence of the matrix elements on the isospin is trivial and after averaging over the angle [see Eq. (14)] the total potential can be written as

$$v_{pp}(k,p) = \frac{1}{8E(k)E(p)kp}\sum_i \chi_i(A_i(k,p)\Theta_i(k,p) + B_i(k,p)\Phi_i(k,p) + C_i(k,p)\Upsilon_i(k,p)), \tag{A3}$$

where $i=\sigma,\omega,\pi,\rho$, the functions $\Theta_i(k,p)$, $\Phi_i(k,p)$, and $\Upsilon_i(k,p)$ are defined by

$$\Theta_i(k,p) = \ln\frac{(k+p)^2+m_i^2}{(k-p)^2+m_i^2}\frac{(k-p)^2+\Lambda_i^2}{(k+p)^2+\Lambda_i^2} \tag{A4}$$

$$\Phi_i(k,p) = (\Lambda_i^2-m_i^2)\left[\frac{1}{(k+p)^2+\Lambda_i^2}-\frac{1}{(k-p)^2+\Lambda_i^2}\right] \tag{A5}$$

$$\Upsilon_i(k,p) = (\Lambda_i^2-m_i^2)^2\ln\frac{(k+p)^2+\Lambda_i^2}{(k-p)^2+\Lambda_i^2}, \tag{A6}$$

the coefficients $A_i(k,p)$, $B_i(k,p)$, and $C_i(k,p)$ are given in Table II, and the functions $a(k,p)$, $b(k,p)$, and $c(k,p)$ are defined as

$$a(k,p) = 4M^{*2}-(E_k-E_p)^2 \tag{A7}$$

$$b(k,p) = 4(2E_kE_p-M^{*2}) \tag{A8}$$

$$c(k,p) = 4E_kE_p+(E_k+E_p)^2. \tag{A9}$$

[1] A. Bohr, B. R. Mottelson, and D. Pines, Phys. Rev. **110**, 936 (1958).
[2] P. Ring and P. Schuck, *The Nuclear Many-Body Problem* (Springer Verlag, Heidelberg, 1980).
[3] J. Decharge and D. Gogny, Phys. Rev. C **21**, 1568 (1980).
[4] J. Dobaczewski, H. Flocard, and J. Treiner, Nucl. Phys. **A422**, 103 (1984).
[5] R. Brockmann and R. Machleidt, Phys. Rev. C **42**, 1965 (1990).
[6] Y. K. Gambhir, P. Ring, and A. Thimet, Ann. Phys. (N.Y.) **198**, 132 (1990).
[7] G. F. Bertsch and H. Esbenson, Ann. Phys. (N.Y.) **209**, 327 (1991).
[8] J. Meng and P. Ring, Phys. Rev. Lett. **77**, 3963 (1996).
[9] J. Meng, W. Pöschl, and P. Ring, Z. Phys. A **358**, 123 (1997).
[10] W. H. Dickhoff, Phys. Lett. B **210**, 15 (1988).
[11] A. B. Migdal, *Theory of Finite Fermi Systems, Applications to Atomic Nuclei* (Wiley Interscience, New York, 1967).
[12] J. M. C. Chen, J. W. Clark, R. D. Davé, and V. V. Khodel, Nucl. Phys. **A555**, 59 (1993).
[13] M. Baldo, J. Cugnon, A. Lejeune, and U. Lombardo, Nucl. Phys. **A515**, 409 (1990).
[14] D. Bailin and A. Love, Phys. Rep. **107**, 325 (1984).
[15] H. Kucharek and P. Ring, Z. Phys. A **339**, 23 (1991).
[16] L. P. Gorkov, Sov. Phys. JETP **34**, 505 (1958).
[17] F. B. Guimaraes, B. V. Carlson, and T. Frederico, Phys. Rev. C **54**, 2385 (1996).
[18] M. Matsuzaki, Phys. Rev. C **58**, 3407 (1998).

[19] H. Kucharek, P. Ring, P. Schuck, R. Bengtsson, and M. Girod, Phys. Lett. B **216**, 249 (1989).
[20] R. Machleidt, Adv. Nucl. Phys. **19**, 189 (1989).
[21] P. Ring, Prog. Part. Nucl. Phys. **37**, 193 (1996).
[22] J. Boguta and A. R. Bodmer, Nucl. Phys. **A292**, 413 (1977).
[23] P. G. Reinhard, M. Rufa, J. Maruhn, W. Greiner, and J. Friedrich, Z. Phys. A **323**, 13 (1986).
[24] F. J. W. Hahne and P. Ring, Phys. Lett. B **259**, 7 (1991).